Plasma Physics Reports, Vol. 24, No. 2, 1998, pp. 148–153. From Fizika Plazmy, Vol. 24, No. 2, 1998, pp. 169–176.

PARTICLE DIAGNOSTICS

Measurement of Fast Ion Dynamics in a High Temperature Plasma[1]

D. J. Den Hartog, A. F. Almagri, J. T. Chapman, G. Fiksel, C. C. Hegna, and S. C. Prager

Department of Physics, University of Wisconsin, Madison, WI 53706 USA

Abstract—Measurement of fast changes and fluctuations in ion flow and/or temperature is critical to understanding a diversity of plasma phenomena. We have developed a high-resolution spectrometer to measure impurity ion temperatures and flow velocities in high-temperature plasmas with 250 kHz bandwidth. This device is actually a *duo*-spectrometer: measurements from two different chordal views of the plasma can be made simultaneously. All 32 spectral channels on the exit plane of the duo-spectrometer are read out and digitized at 1 MHz in parallel to achieve high time resolution. We have obtained these key results: (1) The toroidal velocity fluctuations of the plasma are coherent with the large-scale magnetic tearing modes; during a sawtooth event the scalar product of $\tilde{v}_\phi$ and $\tilde{B}_r$ is similar to that expected for the MHD dynamo electromotive force. (2) Toroidal plasma flow closely tracks the toroidal rotation of the magnetic tearing modes, including the fast changes that occur during sawtooth and locking events.

I. INTRODUCTION

Knowledge of the fast dynamics of ion flow and temperature is crucial to the development of an understanding of a wide variety of the phenomena that occur in a high-temperature plasma. For example, the L-to-H confinement transition in tokamaks is accompanied or caused by a fast transition in the plasma flow profile [1]. Flow and temperature fluctuations play key roles in transport [2] and the MHD dynamo [3]. Sawtooth and locking events are often accompanied by fast changes in the plasma flow and flow profile [4]. In the Reversed-Field Pinch (RFP), fast ion heating occurs coincident with the sawtooth events [5]. In order to study these types of phenomena in the Madison Symmetric Torus (MST) RFP, we developed a flexible grating spectrometer to record Doppler broadened and shifted impurity ion emission. Our device is actually a *duo*-spectrometer: measurements from two different chordal views of the plasma can be made simultaneously via two fused silica fiber optic bundles. High time resolution (250 KHz measurement bandwidth) is achieved by reading out and digitizing all spectral channels in parallel.

Our duo-spectrometer has been operational for several years on the MST RFP, used primarily to study the flow fluctuations responsible for the MHD dynamo and a diversity of phenomena related to plasma flow, magnetic mode rotation, and sawtooth events. MST is a large RFP with major radius $R = 1.5$ m, minor radius $a = 0.5$ m, a thick (5 cm) aluminum conducting shell [6], with standard discharge parameters $T_e = 230$ eV, $n_e = 1.0 \times 10^{19}$ m^{-3}, and $\tau_E = 1.1$ ms at $I_p = 340$ kA. Usually, Doppler measurements are made of the 227.1 nm C V emission (representative of the core ions) or the 229.7 nm C III emission (representative of the edge ions). These two lines are distinct and exhibit a line profile in MST that is dominated by thermal broadening. The few percent carbon impurity in the hydrogen plasma originates mainly from small graphite bumper limiters.

Passive Doppler spectroscopy has been applied to measure the dynamics of the impurity ions in many high-temperature plasmas. A typical approach employs an intensified linear photodiode or CCD array at the exit plane in a highly dispersive spectrometer [7]. While this type of system has good sensitivity and resolution, typical readout times are ~1 ms. For higher time resolution, multiple discrete detectors are used to record several spectral elements simultaneously at high sampling rates. Our duo-spectrometer is representative of this principle and is unique in specific application and achievement, but there are other instruments with parallel readout and good time resolution [8]. Beginning to be exploited is application of high time resolution spectrometers with large etendue and good spectral resolution to charge-exchange recombination spectroscopy [9]. Such a diagnostic provides both time and spatial resolution, since impurity emission is collected from only a small volume of the plasma rather than a chord average.

This paper is organized as follows. The next section is a brief description of our instrument, which we call the Ion Dynamics Spectrometer (IDS). This section will also address some measurement issues, such as the relationship of impurity and majority species flow velocity. The third section will describe our measurements of flow velocity fluctuations and issues related to the study of the MHD dynamo in MST. The fourth sec-

[1]This article was submitted by the authors in English.

1063-780X/98/2402-0148$15.00 © 1998 МАИК Наука/Interperiodica Publishing

tion is a short review of results related to plasma flow, magnetic mode rotation, and sawtooth events. The final section is a summary.

II. THE ION DYNAMICS SPECTROMETER

Only a brief description of the IDS is given here, as this system and its calibration have been described in detail elsewhere [10, 11]. Our instrument simultaneously records two chordal views of the plasma, each with 16 spectral wavelength channels (spreading out the Doppler-broadened spectrum over a large number of spectral channels decouples small fluctuations in the line centroid from those in the line width). The basic design of our spectrometer is that of an $f/10$ Czerny-Turner monochromator with 1.0 m focal length. It is equipped with an 1180 g/mm grating blazed at 1000 nm; high dispersion is achieved by using this grating in fifth order when recording the C III and C V lines listed above. The most inexpensive way of optimizing system etendue was to use straight tall entrance slits (one slit above the optical midplane, the other below). The dominant aberration is then line curvature, which is caused by the variation in dispersion that occurs as a function of slit height. As long as the slit is fairly wide and not too tall, such line curvature can be compensated quite well by a simple tilt (0.5° in our case) of a straight slit. The dispersed spectra on the exit plane of the duospectrometer are coupled via fused silica fiber optic bundles to two arrays of 16 photomultiplier tubes each. All 32 photomultiplier tubes are read out and digitized at 1 MHz in parallel. The result is a system which combines good etendue and resolution with the simplicity and flexibility of a fiber-optically coupled single-grating spectrometer. Measurement precision is proportional to the impurity emission photon flux; typically, flow can be measured to a precision of 1 km/s with 10 μs time resolution.

The usual mode of operation of the IDS on MST is to record the toroidal flow velocity with two opposing chordal views, one for the Doppler red shift and the other for the blue. This has the advantage of automatically calibrating for the unshifted line center on the exit plane of the spectrometer, as it is simply the difference between the two views. Once calibrated by such a procedure, one of the views can be moved to record the poloidal velocity, thus providing for simultaneous measurement of the poloidal and toroidal flows.

The fundamental limiting factor of the capability of the IDS system is spatial resolution. Since the IDS collects a chord-integrated view of the impurity line emission, spatial resolution is limited to lengths ≥20% of the minor radius. For example, a convolution of the measured C V emission profile and the toroidal viewing chord of the IDS as installed on MST indicates that most of spectral information of flow and temperature originates between r/a of 0.3 and 0.5. Fortunately, much of the MHD phenomena of interest on MST are spatially large-scale, with wavelengths on the order of $2\pi R/n$ (which, for MST with the dominant toroidal mode number $n = 6$, is about equal to R, the major radius). Thus, the inherent limits of passive spectroscopy increase the difficulty of, but do not render impossible, studies of spatial flow fluctuations.

Since the behavior of the majority ion species (or more specifically, the MHD single-fluid behavior of the plasma) is of greatest interest for our studies, the question naturally arises of how to relate IDS measurements of impurity ion dynamics to such quantities. Since the plasma flow velocity $\mathbf{v} = (m_i\mathbf{v}_i + m_e\mathbf{v}_e)/(m_i + m_e) \approx \mathbf{v}_i$, measurement of the ion flow should be sufficient for an MHD description of the plasma. The relationship of the impurity and majority flows has been explored in detail for tokamaks [12], but a similar analysis has not been done for the RFP, where magnetic field shear is substantial and the poloidal and toroidal magnetic fields are similar in magnitude. However, using some simple assumptions, a basic relationship between impurity and majority flows can be derived. For each species s,

$$\mathbf{v}_s = v_{\|s}\frac{\mathbf{B}}{B} + \frac{\mathbf{E}\times\mathbf{B}}{B^2} + \frac{\mathbf{B}\times\nabla p_s}{n_s q_s B^2}, \qquad (1)$$

where $v_{\|s}$ is the velocity parallel to the magnetic field, $\mathbf{E}$ and $\mathbf{B}$ are the electric and magnetic fields respectively, p_s is the pressure (the prime indicates a radial derivative), n_s is the particle density, and q_s is the charge. For simplicity, we consider the case of two species, majority ions i, and a small population of impurity ions I. To a good approximation, the parallel velocities of these two species are equivalent, because the friction force of majority ions on the impurity ions is dominant (the calculated collisional equilibration time for the carbon impurity ions with the majority protons is approximately 50 μs). Then, for impurity toroidal flow in an RFP, assuming $v_{\theta i}$ to be small (for simplicity),

$$v_{\phi I} = v_{\phi i} + \frac{p_i' B_\theta}{n_i q_i B^2} - \frac{p_I' B_\theta}{n_I q_I B^2}. \qquad (2)$$

The difference in toroidal flows is due to the difference in diamagnetic drifts, since the $\mathbf{E}\times\mathbf{B}$ drifts are identical. In the core of the RFP, the diamagnetic drifts of the impurity species (C^{+4}) and the majority protons are not large compared to the expected $\mathbf{E}\times\mathbf{B}$ drifts; therefore, the core toroidal flows are probably equal to reasonably good approximation. However, the edge impurity species (C^{+2}) has an edge-peaked pressure profile, with positive p_I' just inside $r/a \approx 0.95$ and negative p_I' just outside. Thus, the C^{+2} ion flow may be strongly sheared around $r/a \approx 0.95$. If sufficient spatial resolution was available with an impurity flow diagnostic, this sheared flow profile could be measured. However, the spatial resolution of the IDS is such that the opposing Doppler shifts caused by these local diamagnetic drifts are probably averaged to approximately zero, contributing only

a slight symmetric broadening to the Doppler profile. What remains, then, is the Doppler shift caused by the toroidal flow of the majority species. So, even in the edge plasma, the toroidal flow velocity recorded by the IDS is probably representative of the majority species.

III. MEASUREMENT OF SPATIAL VELOCITY FLUCTUATIONS AND THE MHD DYNAMO IN THE CORE OF MST

A series of experiments has been carried out in MST, both in the edge [13] and the core [14], to measure the MHD dynamo electric field parallel to the equilibrium magnetic field. This dynamo arises from the correlation between the spatially fluctuating flow velocity and the spatially fluctuating magnetic field, expressed as the flux surface-averaged cross product $\langle \tilde{\mathbf{v}} \times \tilde{\mathbf{B}} \rangle$ [3]. In the RFP, the magnetic field, or plasma current parallel to the field, cannot be fully accounted for by the applied toroidal electric field. This is dramatically evident in the outer region of the plasma, where the applied parallel electric field is either zero or actually points in the direction opposite to the observed current. This magnetic field configuration is sustained for times long compared to τ_R, the resistive decay time of the magnetic fields.

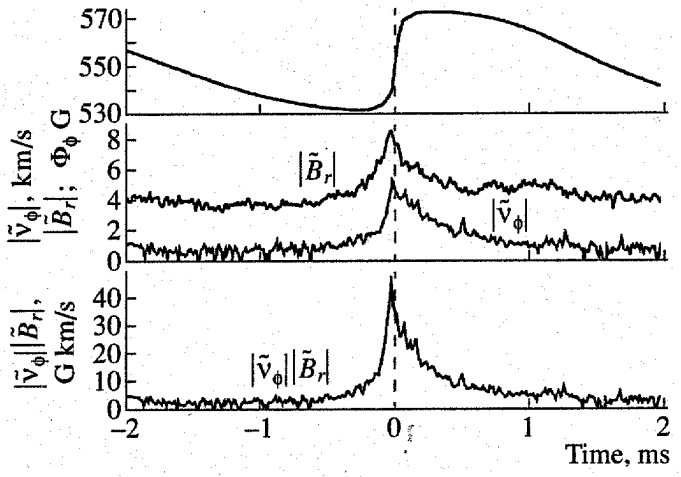

Fig. 1. An ensemble average illustrating the sawtooth change in toroidal flux Φ_ϕ, velocity and magnetic field fluctuations, and the scalar quantity $|\tilde{v}_\phi||\tilde{B}_r|$.

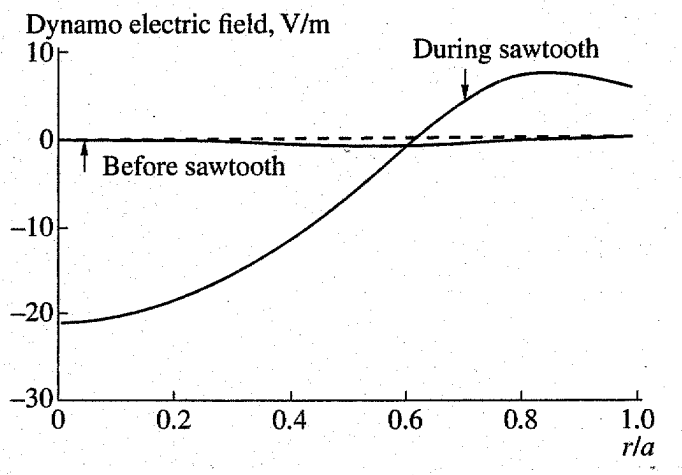

Fig. 2. Ohm's law estimates of the dynamo electric field before and during the sawtooth crash.

Dynamo activity in MST is most clearly manifested by the sawtooth "discrete dynamo" events [15–17]. Sawtooth events occur in MST with periods of 2–6 ms, depending on the plasma parameters. Strong spontaneous magnetic field generation is evident in the sudden increase in toroidal flux Φ_ϕ during a sawtooth crash (at $t = 0$ in Fig. 1). Decreases in the pinch parameter $\Theta \equiv B_\theta(a)/(\Phi_\phi/\pi a^2)$ and the reversal parameter $F \equiv B_\phi(a)/(\Phi_\phi/\pi a^2)$ indicate that, during a crash, the plasma relaxes toward a minimum energy state with a flatter current profile; i.e., current decreases at the core and increases at the edge. Between crashes, a "continuous dynamo" may be operative at a low level.

In order to estimate the level of dynamo activity expected in MST throughout a sawtooth period, we have done parallel Ohm's law modeling of the plasma:

$$E_\parallel = \eta_\parallel J_\parallel - E_{d\parallel} - E_{ind\parallel}, \tag{3}$$

where $E_\parallel$ is the applied parallel electric field, $\eta_\parallel$ is the parallel Spitzer resistivity, $J_\parallel$ is the parallel current density, $E_{d\parallel}$ is the MHD dynamo term $\langle \tilde{\mathbf{v}} \times \tilde{\mathbf{B}} \rangle_\parallel$, and $E_{ind\parallel}$ is the electric field induced by the evolving magnetic field (the current density profile continuously evolves throughout the sawtooth period). The RFP equilibrium appears to be the result of a relaxation to a minimum energy state, during which global magnetic helicity is conserved [18]. For an RFP with finite pressure:

$$\nabla \times \mathbf{B} = \mathbf{J}_\parallel + \mathbf{J}_\perp = \lambda \mathbf{B} - \frac{\nabla p \times \mathbf{B}}{B^2}, \tag{4}$$

where λ is a function of r for a realistic RFP, and $p(r)$ is the pressure profile. MST does not have a complete set of profile diagnostics, but with reasonable assumptions for $T_e(r)$ and $Z_{\text{eff}}(r)$ and measurements of $n_e(r)$, total toroidal plasma current, and edge and average toroidal magnetic field, we obtain estimates of $E_{d\parallel}$ before and during the sawtooth crash (Fig. 2). Irrespective of the details, note that the dynamo electric field is expected to be small between sawteeth, but should be very large during the sawtooth flux generation event.

The MST device is well equipped with arrays of three-axis coil sets distributed toroidally and poloidally inside the vacuum vessel. These are capable of recording mode-resolved magnetic fluctuations up to 250 kHz. Since the tearing modes in the core of MST are global, these edge coils are completely sufficient for recording the magnetic fluctuations associated with the MHD dynamo (we have confirmed this by inserting an

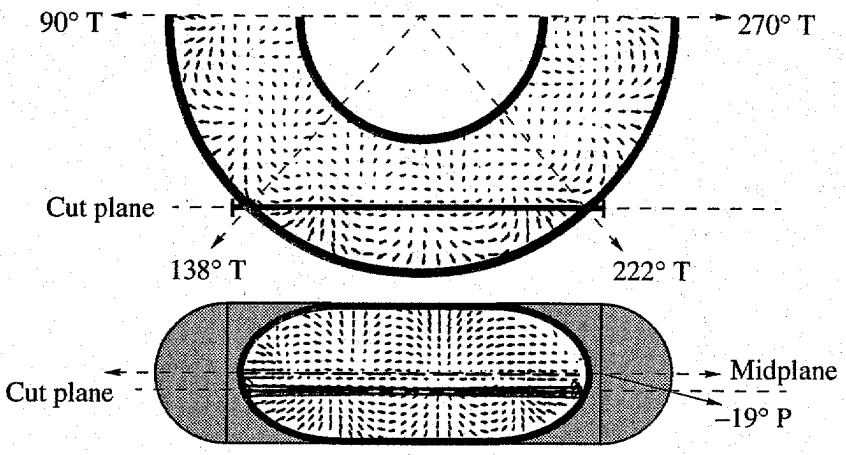

Fig. 3. A graphical illustration of the line integral of an $m = 1$, $n = 6$ ion velocity field as recorded by the IDS. The ion velocity field shown is for illustration only and should not be taken as representative of the actual vector field in MST.

armored probe containing pickup coils deep into the plasma). We are measuring the velocity fluctuations in the core of MST spectroscopically with the IDS.

The velocity fluctuations in the core plasma and the core tearing mode magnetic fluctuations exhibit coherence around 15 kHz, indicating that both these quantities are large-scale MHD fluctuations of the order of the plasma size. (This coherence frequency is measured in the frame of the laboratory; typically, in MST, the plasma exhibits an equilibrium rotation, which causes spatial fluctuations in the frame of the plasma to be recorded as frequency fluctuations in the lab frame). Both velocity and magnetic fluctuations grow in magnitude and peak at the sawtooth crash, indicating enhanced dynamo activity (Fig. 1). The scalar product of $\tilde{v}_\phi$ and $\tilde{B}_r$ exhibits the sawtooth cycle time variation expected for the dynamo electromotive force in MST, although away from the sawtooth event, this scalar product is larger than the dynamo electromotive force predicted by the Ohm's law calculations. However, the full picture requires comparison of the Ohm's law predictions to the actual dynamo product $\langle \tilde{\mathbf{v}} \times \tilde{\mathbf{B}} \rangle$, the magnitude of which is dependent not only on the magnitude of the individual components of velocity and magnetic field, but also on their phase relationship.

Measurement of the phase of the spatial velocity fluctuation in an MST plasma is complicated, because the IDS records a chord-integrated view of the flow pattern. Figure 3 is a graphical illustration of the line integral of a possible ion velocity field as recorded by the spectrometer. It is straightforward to show that this observation geometry strongly attenuates the IDS signal from flow patterns with a near-integer number of wavelengths along the viewing chord. Fortunately, for the particular viewing geometry we have on MST, flow patterns with the expected $m = 1$, $n = 5$–8 structure should provide a measurable signal to the IDS. However, there is a substantial phase shift between the fluctuating velocity signal recorded by the IDS and the actual fluctuation in the ion velocity as the plasma rotates by a fixed toroidal location in MST. In general, this recorded phase shift depends on the details of the impurity emission profile and the exact structure of the flow patterns. The expected flow pattern structure can, in principle, be computationally predicted by toroidal resistive 3-dimensional MHD simulation, but doing so is complex and time-consuming. However, progress can be made using simple approximations. Assume that the magnetic field and velocity fluctuations are single helicity perturbations that rotate in the lab frame with frequency ω:

$$\tilde{B} = \tilde{B}_0 \sin(m\theta - n\phi + \omega t), \tag{5}$$

$$\tilde{v} = \tilde{v}_0 \sin(m\theta - n\phi + \omega t + \delta), \tag{6}$$

where δ is the actual phase difference between the fluctuations. Assume that this velocity fluctuation is localized to a mode rational surface. Then the $\tilde{v}_{\mathrm{IDS}}$ recorded by the IDS originates from the two toroidally symmetric points at which the viewing chord intersects the rational surface (Fig. 3):

$$\begin{aligned}\tilde{v}_{\mathrm{IDS}} &= \frac{\tilde{v}_0}{2}\{\sin[m\theta_{rs} - n(\phi_{rs} + \phi_0) + \omega t + \delta] \\ &\quad + \sin[m\theta_{rs} - n(\phi_0 + \phi_{rs}) + \omega t + \delta]\} \\ &= \tilde{v}_0 \sin[m\theta_{rs} - n\phi_0 + \omega t + \delta]\cos[n\phi_{rs}],\end{aligned} \tag{7}$$

where θ_{rs} and ϕ_{rs} are the angular locations of the intersections of the two opposing viewing chords with the rational surface and ϕ_0 is the toroidal angle midway between the two viewing ports. As can be seen from this equation, the toroidal location of the intersections does not affect the measured phase but is only an attenuation factor on $\tilde{v}_{\mathrm{IDS}}$. However, the poloidal location of the intersections does affect the measured phase. This is a problem, because θ_{rs} is difficult to estimate

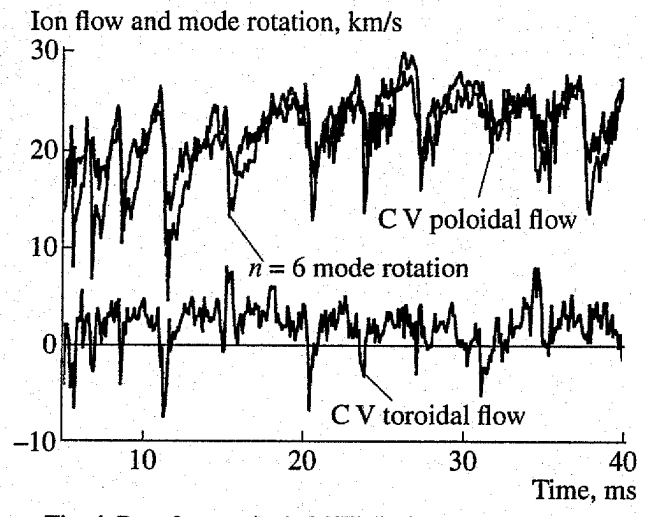

Fig. 4. Data from a single MST discharge, showing the toroidal and poloidal plasma flow velocity and the $n = 6$ mode phase velocity.

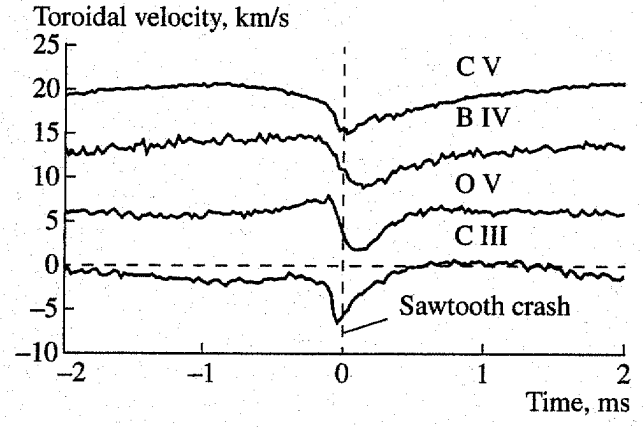

Fig. 5. A qualitative illustration of the flow profile over a sawtooth period in MST, showing substantial shear from core to edge. C V is representative of the core plasma, C V of the edge, with the other two impurities between core and edge.

and varies by nearly $\pi/2$ depending on the radial location of the rational surface.

Fortunately, this problem can be solved by selecting the proper viewing chords with which to record IDS velocity fluctuation data. Up to now, we have simultaneously collected light from two toroidal viewing chords viewing the same chord in opposite directions (Fig. 3); this amounts to two implementations of the viewing geometry described by (7). In the near future, we will move one chord slightly above the midplane at +19 poloidal angle, leaving the other at −19 poloidal angle. If both chords view in the same direction, then from (7),

$$\begin{aligned}\tilde{v}_{\mathrm{IDS}} &= \frac{\tilde{v}_0}{2}\{\sin[m\theta_{rs} - n\phi_0 + \omega t + \delta]\cos[n\phi_{rs}] \\ &\quad + \sin[-m\theta_{rs} - n\phi_0 + \omega t + \delta]\cos[n\phi_{rs}]\} \\ &= \tilde{v}_0 \sin[-n\phi_0 + \omega t + \delta]\cos[m\theta_{rs}]\cos[n\phi_{rs}].\end{aligned} \tag{8}$$

Both the toroidal and poloidal intersections with the rational surface are then only attenuation factors and do not affect the measured phase of the toroidal velocity fluctuations. For a poloidal viewing chord, the $\tilde{v}_{\mathrm{IDS}}$ recorded by the IDS is

$$\begin{aligned}\tilde{v}_{\mathrm{IDS}} &= \frac{\tilde{v}_0}{2}\{\sin[m(\theta_{rs} + \theta_0) - n\phi_0 + \omega t + \delta] \\ &\quad + \sin[m(\theta_0 + \theta_{rs}) - n\phi_0 + \omega t + \delta]\} \\ &= \tilde{v}_0 \sin[m\theta_0 - n\phi_0 + \omega t + \delta]\cos[m\theta_{rs}].\end{aligned} \tag{9}$$

In this case also, the phase of the measured poloidal velocity fluctuations is not affected by the angular locations of the intersections with the rational surface. So, by using these two schemes, we will be able to measure two important components of the dynamo cross product, $\langle \tilde{v}_\phi \tilde{B}_r \rangle$ and $\langle \tilde{v}_\theta \tilde{B}_r \rangle$. In the near future, we will also be constructing appropriate radial viewing ports for the IDS in order to obtain the $m = 1$ component of the radial velocity fluctuations in order to measure $\langle \tilde{v}_r \tilde{B}_\phi \rangle$ and $\langle \tilde{v}_r \tilde{B}_\theta \rangle$.

IV. PLASMA FLOW AND MAGNETIC MODE LOCKING

In addition to fluctuation studies, the IDS is useful for recording the equilibrium plasma flow in MST, and particularly its relationship to magnetic mode locking. Figure 4 is data from a single MST discharge, showing the toroidal and poloidal plasma flow velocity and the $n = 6$ mode phase velocity. Note the close correspondence between v_ϕ and $v_{n=6}$, even during sawtooth events. We are pursuing ongoing studies of the relationship of the plasma flow and mode rotation [4], with focus on the torques that affect the plasma and modes. Electromagnetic torques on the resistive tearing modes in the core of MST ($m = 1$, $n = 5$–8) are an important determinant of rotation and locking. Such torques may be classified into two types: external, arising from the interaction of a vacuum field error with the core modes [19, 20]; and internal, from nonlinear interaction of modes at the reversal surface (e.g., $m = 0$, $n = 1$) with the core modes [21]. Viscous coupling between the tearing mode islands and the plasma appears to be large in MST [22]. In addition to such viscous torques, there may be an acceleration force arising from the fluid stress term, $\langle \tilde{\mathbf{v}} \cdot \nabla \tilde{\mathbf{v}} \rangle$ [23]. As can be seen from Fig. 1, $\langle \tilde{\mathbf{v}} \cdot \nabla \tilde{\mathbf{v}} \rangle$ peaks during the sawtooth crash, suggesting that this term, which generates equilibrium plasma flow, may be large during a sawtooth.

The flow profile, both equilibrium and during a sawtooth, exhibits substantial radial shear in MST. A rough picture of the flow profile has been constructed by measuring the Doppler shift of various impurity ion states; the toroidal plasma flow appears to slow down and even reverse direction near the edge (Fig. 5). The oppositely

directed flow of the edge plasma may be due to the fact that the radial electric field E_r changes sign near the reversal surface [24]. The magnitude of this reverse velocity at the edge can be dramatically increased by applying a negative bias to the edge plasma. Such a bias even reverses the direction of the core plasma, presumably through viscous coupling. The radial shear in the velocity profile does increase during biasing. This coupling of edge biasing to core rotation can also be used to unlock and accelerate locked discharges [25].

V. SUMMARY

We have developed a duo-spectrometer, which is used on the MST RFP to precisely measure equilibrium and fluctuating plasma flow. This instrument records Doppler-shifted impurity line emission from both toroidal and poloidal viewing chords. Even with the limitations imposed by chord-integrated measurement of impurity ions, with the careful measurement techniques described above, we are able to accurately measure the flow behavior of the plasma. We have demonstrated that the toroidal flow velocity fluctuations peak during a sawtooth event when MHD dynamo activity is expected to be largest and when toroidal flux is generated. Plasma flow and core tearing mode rotation exhibit close coupling and complex behavior involving electromagnetic and viscous torques and possibly velocity stress forces.

ACKNOWLEDGMENTS

The entire MST group contributed to the work presented in this paper. This work is supported by the United States Department of Energy.

REFERENCES

1. Burrell, K.H., *Phys. Plasmas*, 1997, vol. 4, p. 1499.
2. See, for example, Prager, S.C., *Plasma Phys. Controlled Fusion*, 1990, vol. 32, p. 903.
3. Ortolani, S. and Schnack, D.D., *Magnetohydrodynamics of Plasma Relaxation*, Singapore: World Scientific, 1993, pp. 95–127.
4. Den Hartog, D.J., Almagri, A.F., Chapman, J.T., Fonck, R.J., Hegna, C.C., Ji, H., Prager, S.C., and Sarff, J.S., *Phys. Plasmas*, 1995, vol. 2, p. 2281.
5. Scime, E., Cekic, M., Den Hartog, D.J., Hokin, S., Holly, D.J., and Watts, C., *Phys. Fluids B*, 1992, vol. 4, p. 4062.
6. Dexter, R.N., Kerst, D.W., Lovell, T.W., Prager, S.C., and Sprott, J.C., *Fusion Technol.*, 1991, vol. 19, p. 131.
7. See, for example, Carolan, P.G., Conway, N.J., Bunting, C.A., Leahy, P., O'Connell, R., Huxford, R., Negus, C.R., and Wilcock, P.D., *Rev. Sci. Instrum.*, 1997, vol. 68, p. 1015; or Den Hartog, D.J., and Holly, D.J., *Rev. Sci. Instrum.*, 1997, vol. 68, p. 1036.
8. See, for example, Carolan, P.G. and O'Connell, R., *Rev. Sci. Instrum.*, 1995, vol. 66, p. 1184.
9. Evensen, H.T., Durst, R.D., Fonck, R.J., Paul, S.F., and Scott, S.D., *Bull. Am. Phys. Soc.*, 1995, vol. 40, p. 1871.
10. Den Hartog, D.J. and Fonck, R.J., *Rev. Sci. Instrum.*, 1994, vol. 65, p. 3238.
11. Chapman, J.T. and Den Hartog, D.J., *Rev. Sci. Instrum.*, 1997, vol. 68, p. 285.
12. Kim, Y.B., Diamond, P.H., and Groebner, R.J., *Phys. Fluids B*, 1991, vol. 3, p. 2050.
13. Ji, H., Prager, S.C., Almagri, A.F., Sarff, J.S., Yagi, Y., Hirano, Y., Hattori, K., and Toyama, H., *Phys. Plasmas*, 1996, vol. 3, p. 1935.
14. Den Hartog, D.J., Almagri, A.F., Cekic, M., Chapman, B.E., Chapman, J.T., Chiang, C.-S., Craig, D., Crocker, N.C., Fiksel, G., Fontana, P.W., Hansen, A.K., Hegna, C.C., Ji, H., Lanier, N.E., Mirus, K.A., Prager, S.C., Sarff, J.S., Sprott, J.C., Stoneking, M.R., and Uchimoto, E., Reducing and Measuring Fluctuations in the MST RFP: A Five-fold Enhancement of Energy Confinement and Measurement of the MHD Dynamo, *Proc. Sixteenth IAEA Fusion Energy Conf.*, Montreal, 1996 (in press).
15. Watt, R.G. and Nebel, R.A., *Phys. Fluids*, 1983, vol. 26, p. 1168.
16. Hokin, S., Almagri, A., Assadi, S., Beckstead, J., Chartas, G., Crocker, N., Cudzinovic, M., Den Hartog, D., Dexter, R., Holly, D., Nebel, R., Prager, S., Rempel, T., Sarff, J., Scime, E., Shen, W., Spragins, C., Sprott, C., Starr, G., Stoneking, M., and Watts, C., *Phys. Fluids B*, 1991, vol. 3, p. 2241.
17. Hegna, C.C., Prager, S.C., Gimblett, C.G., and Thyagaraja, A., *Bull. Am. Phys. Soc.*, 1995, vol. 40, p. 1874.
18. Taylor, J.B., *Phys. Rev. Lett.*, 1974, vol. 33, p. 1139; *Rev. Mod. Phys.*, 1986, vol. 58, p. 741.
19. Zohm, H., Kallenbach, A., Bruhns, H., Fussmann, G., and Kluber, O., *Europhys. Lett.*, 1990, vol. 11, p. 745.
20. Fitzpatrick, R., *Nucl. Fus.*, 1993, vol. 33, p. 1049; Fitzpatrick, R., Hastie, R.J., Martin, T.J., and Roach, C.M., *Nucl. Fusion*, 1993, vol. 33, p. 1533.
21. Hegna, C.C., *Phys. Plasmas*, 1996, vol. 3, p. 4646.
22. Yokoyama, M., Callen, J.D., and Hegna, C.C., *Nucl. Fusion*, 1996, vol. 36, p. 1307.
23. Wainwright, J.P., Haines, M.G., and Gimblett, C.G., *Plasma Phys. Controlled Fusion*, 1995, vol. 37, p. 1449.
24. Chiang, C.-S., Almagri, A.F., Fiksel, G., Giannone, L., Ji, H., Prager, S., Sarff, J., Stoneking, M., and Thomas, M., *Bull. Am. Phys. Soc.*, 1995, vol. 40, p. 1753.
25. Almagri, A.F., Chapman, J.T., Chiang, C.-S., Den Hartog, D.J., Mirus, K.A., Prager, S.C., and Sarff, J.S., *Bull. Am. Phys. Soc.*, 1995, vol. 40, p. 1753.